Supplementary Material
for
In-silico Screening of Pt-Based Bimetallic Alloy Catalysts Using Ab Initio Microkinetic Modelling for Non-Oxidative Dehydrogenation of Ethanol to Produce Acetaldehyde

Fatima Jalid[1,2,*], Tuhin S. Khan[1,*,$], M. Ali Haider[1,$]
[1]Renewable Energy and Chemicals Laboratory,
Department of Chemical Engineering,
Indian Institute of Technology Delhi, Hauz Khas, Delhi, 110016, India.
[2]Department of Chemical Engineering, National Institute of Technology Srinagar,
Srinagar, Jammu and Kashmir, 190006, India.
[$] Corresponding Authors Email: tuhinsk@iitd.ac.in, haider@iitd.ac.in
Fax: +91-11-2658-2037; Tel: +91-11-26591016
*Equal first author contribution

1 Methodology

The MKM was executed from reaction energetics of the elementary steps for the ethanol NODH reaction on the stepped sitesof the transition metal catalysts viz. Ag, Au, Cu, Co, Ni, Pd, Pt, Rh, Ru and Re. The MKM was based on the previous study on the non-oxidative ethanol dehydrogenation (NODH) of ethanol on transition metal catalysts and Cu and Ni alloys [1]. The stepped surfaces of Pt_3B bimetallics with AA and AB surface termination have been studied herein; Pt being alloyed with transition metals viz. Au, Ag, Cu, Pd, Rh, Ni, Co, Zn, Hf, Nb, Sc, Ta, Ti, V, Y, Zr; and p-block elements viz. Sn, Ga, Ge, Al, Pb, Sb, As, Tl, La.

Steady state kinetics of the elementary reaction steps were determined using the mean field approach, with no assumptions of a rate determining step. The steady-state solutions of the governing differential equations were found using a multi-dimensional Newton's root finding method from the python mpmath library in CatMAP. The model used frozen adsorbate approximation [2, 3], neglecting any entropy change in the reactions taking place on the surface. The model used two separate sites, one for all the adsorbates and the other for hydrogen, owing to the as hydrogen was unlikely to compete with the other adsorbates owing to its small size [4]. The number of hydrogen sites were considered to be equal to the step sites. The microkinetic model was solved for reaction conditions T = 423 K, with 0.01% conversion of ethanol and 1 bar of ethanol.

Binding energies of the adsorbed species, transition state and gas phase species used in the model were obtained from CatApp [5] and previous studies [1, 4, 6–9] based on DFT calculations and microkinetic models of ethanol over the transition metals.

2 Selectivity

The NODH of ethanol yields acetaldehyde as the major product, and ethylene as a byproduct. All the alloys screened in the MKM showed absolute selectivity towards the formation of acetaldehyde as shown in Figure SI-1.

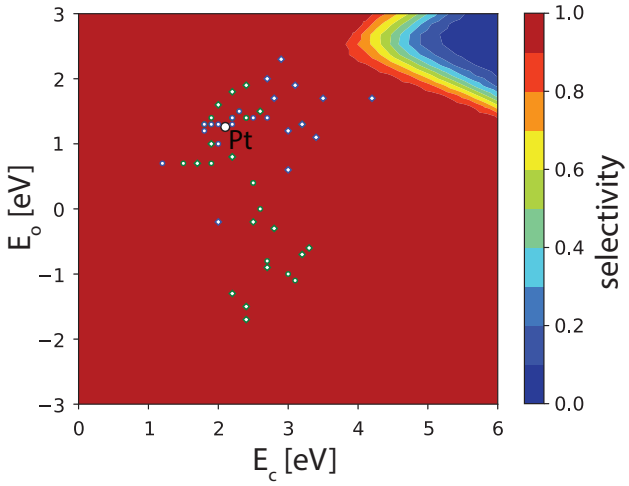

Figure SI-1: Selectivity for acetaldehyde over Pt_3B alloys (blue circle and blue diamond represent the AA and AB termination of p-block element based Pt alloys, and green circle and green diamond represent the AA and AB termination of transition metal based Pt alloys)

3 Coverage

In order to gain insights into the activity trends of NODH reaction, we have studied the coverages of various adsorbate species on the Pt alloys. Figure SI-2 shows the coverage of CH_3CH_2O, CH_3CHO, CH_3CO and CH_3CH_2 on all the alloys of Pt studied herein. The coverage of this species is depicted in Figure SI-2(a). Of the AA termination p-block element alloys, Pt_3Ge and Pt_3Sn exhibited complete and partial coverage of ethoxy species, respectively. All the AB termination p-block element alloys of Pt show coverage of CH_3CH_2O except Pt_3La. Pt_3La has the lowest turnover of acetaldehyde of these alloys. This implies that the species exhibiting a high coverage of ethoxy have a high turnover of acetaldehyde, implying that this is an important intermediate towards the aldehyde production. The AA terminal of Pt_3Ni and AB of Pt_3Cu, are the transition metal based alloys that show partial coverage of CH_3CH_2O. The coverage of the species CH_3CHO is shown in Figure SI-2(b). None of AA termination p-block element based alloys lied in this zone. Pt_3La and Pt_3Al are the only AB termination of p-block element transition metal based Pt alloys that show slight coverage of CH_3CHO. Amongst the transition metal based alloys, the AA terminal of Pt_3V, Pt_3Nb, and Pt_3Ta are completely covered by CH_3CHO. AA surface terminal of Pt_3Ti has a partial coverage of this adsorbed species. The AB termination transition metal based Pt alloys that were covered by this species are Pt_3Y, Pt_3Sc, Pt_3Hf, Pt_3Zr, Pt_3Ti, Pt_3V, Pt_3Ta, and Pt_3Nb. All of these show complete coverage of CH_3CHO. However, these metals have a turnover of less than $10^{-3}s^{-1}$ for the production of acetaldehyde. From this observation, it can be concluded that alloys showing high coverage of CH_3CHO do not have high aldehyde production rate. The -H abstraction of CH_3CHO produced CH_3CO, the coverage of which is shown in Figure SI-2(c). The AA surface terminal Pt alloys with p-block elements that show CH_3CO coverage are Pt_3La, Pt_3As, Pt_3Cd, Pt_3Tl, Pt_3In, Pt_3Al, Pt_3Pb, Pt_3Sb and Pt_3Ga.

All of these have absolute coverage of CH_3CO except Pt_3Sb and Pt_3Ga. Pt_3La is the only AB termination of p-block element alloys that shows coverage of CH_3CO. Of the AA termination

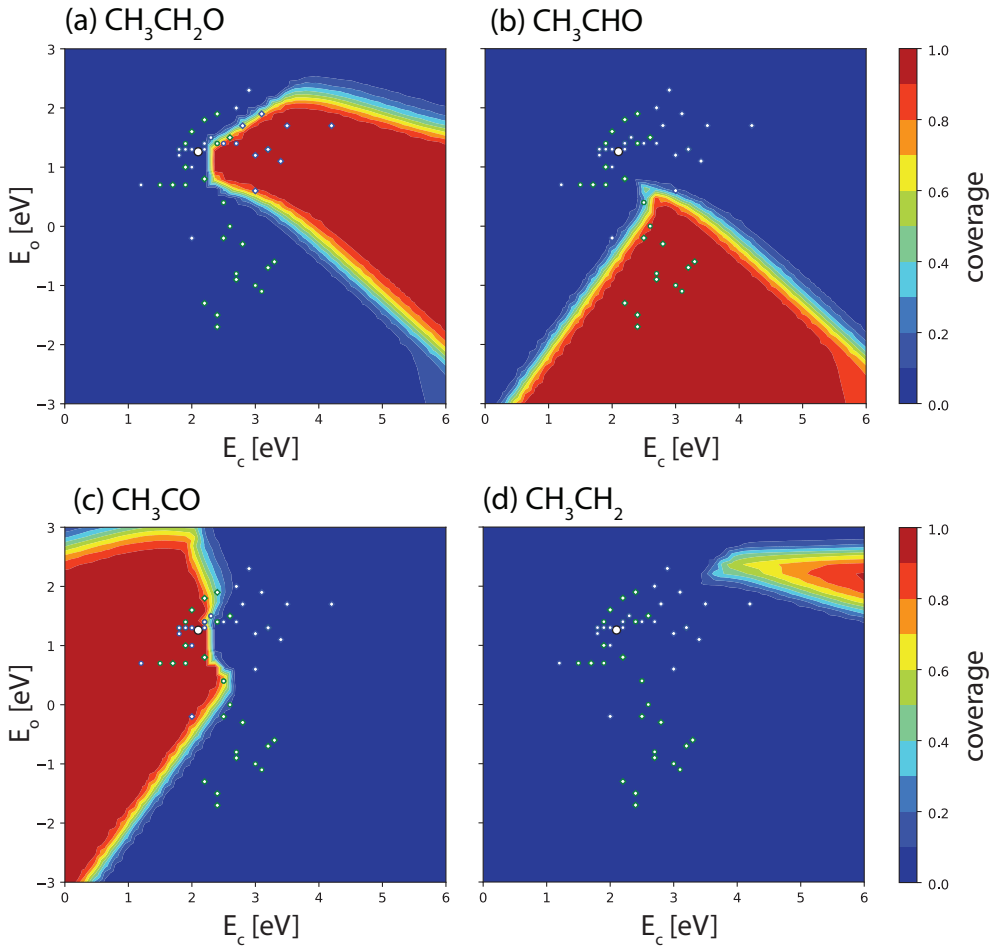

Figure SI-2: Coverages of (a) CH_3CH_2O, (b) CH_3CHO, (c) CH_3CO, (d) CH_3CH_2 over Pt_3B alloys (blue circle and blue diamond represent the AA and AB termination of p-block element based Pt alloys, and green circle and green diamond represent the AA and AB termination of transition metal based Pt alloys)

of transition metal alloys, Pt_3Y, Pt_3Pd, Pt_3Ag, Pt_3Au and Pt_3Rh exhibited complete coverage of CH_3CO whereas Pt_3Sc had partial coverage of this species. The AB surface terminal of the transition metal alloys Pt_3Rh, Pt_3Ni, Pt_3Co, Pt_3Pd are completely covered by CH_3CO and that of Pt_3Ag, and Pt_3Au show partial coverage. These alloys lie to the left of the top of the acetaldehyde volcano plot. None of the alloys screened are covered by CH_3CH_2 [Figure SI-2(d)], which can explain the fact that the turnover of ethylene is very low on these, as ethylene is formed of the dehydrogenation of this specie. From the coverage plots shown in Figure SI-2, it can be concluded that the alloys that have a high coverage of ethoxy species have a high acetaldehyde turnover whereas those that have CH_3CHO and CH_3CO coverage do not have high aldehyde production.

4 CatMAP Input File

A sample input file for NODH of alcohols is shown underneath. *_s represents a free step site (211), *_h represents the hydrogen site. Not all the reactions are listed in the sample.

```
rxn_expressions = [

'CH3CH2OH_g + *_s + *_h <-> H-CH3CHOH_s + *_h -> CH3CHOH_s + H_h',
'CH3CHOH_s + *_h -> CH3CHO-H_s + *_h -> CH3CHO_s + H_h',
'CH3CH2OH_g + *_s + *_h <-> CH3CH2O-H_s + *_h -> CH3CH2O_s + H_h',
'CH3CH2O_s + *_h <-> H-CH3CHO_s + *_h -> CH3CHO_s + H_h',
'CH3CHO_s -> CH3CHO_g + *_s',
  ]

surface_names = ['Pt', 'Ag', 'Au', 'Co', 'Ni', 'Cu', 'Ru', 'Rh', 'Pd', 'Re']

descriptor_names = ['C_s','O_s']

descriptor_ranges = [[0.0, 6.0],[-3.0, 3.0]]

temperature = 423

resolution = 20

species_definitions = {}
species_definitions['CH3CH2OH_g'] = {'pressure':1}
species_definitions['CH4_g'] = {'pressure':0}
species_definitions['CO_g'] = {'pressure':0}
species_definitions['CO2_g']={'pressure':0}
species_definitions['H2_g'] = {'pressure':0}
species_definitions['H2O_g'] = {'pressure':0}
species_definitions['CH2CH2_g'] = {'pressure':0}
species_definitions['CH3CHO_g'] = {'pressure':0.0001}

species_definitions['s'] = {'site_names': ['211'], 'total':1.0}
species_definitions['h'] = {'site_names': ['211'], 'total':1.0}

scaling_constraint_dict = {
 'C_s':['+',0,None],
 'O_s':[0,'+',None],
 'H-CH3CHOH_s':'final_state',
 'CH3CHO-H_s':'final_state',
 'CH3CH2O-H':'final_state',
 'H-CH3CHO_s':'final_state',
                           }

#Define default fixed entropy gas entropies
fixed_entropy_dict = {'H2_g':0.00135,
        'H2O_g':0.0018884,
        'CH3CH2OH_g':0.0028162,
        'CH2CH2_g':0.00227392134,
        'CH4_g':0.0018637,
        'CO_g':0.0019766,
        'CO2_g':0.0021379,
        'CH3CHO_g':0.0027356497,
        'other':0.002,
        }

data_file = 'MKM.pkl'

input_file = 'energies.txt'

gas_thermo_mode = "fixed_entropy_gas"
adsorbate_thermo_mode = "frozen_adsorbate"

decimal_precision = 120

tolerance = 1e-100

max_rootfinding_iterations = 100
```

5 Descriptor Energies and Alloy Prices

The binding energies of cabron and oxygen on the Pt-based alloys used in the model are listed in Table SI-1. The alloy prices are also given in Table SI-1, which have been calculated considering 3:1 ratio of Pt with the alloying metal. The prices of the each metal and the binding energies are taken from previous work conducted on the in-silico screening for methane steam reforming process [10]. The formula for calculation of alloy price as used herein is:

Price of Pt_3B Alloy = [0.75 * Price of Pt ($/kg) * Molar mass of Pt (kg/kmol)] + [0.25 * Price of B ($/kg) * Molar mass of B (kg/kmol)]

Table SI-1: Descriptor energies and alloy prices over the Pt based alloys

Alloy	Surface Termination	C [eV]	C [eV]	Price [$/kmol]
Pt_3Au	AB	2.2	1.8	21740950
Pt_3Au	AA	1.8	1.3	21740950
Pt_3Ag	AB	2.4	1.9	19044900
Pt_3Ag	AA	1.8	1.3	19044900
Pt_3Cu	AB	2.6	1.5	19013810
Pt_3Cu	AA	2.2	1.4	19013810
Pt_3Pd	AB	2.0	1.6	20558245
Pt_3Pd	AA	1.9	1.3	20558245
Pt_3Rh	AB	1.7	0.7	22360000
Pt_3Rh	AA	1.9	1.4	22360000
Pt_3Ni	AB	1.9	1.0	19013636
Pt_3Ni	AA	2.3	1.5	19013636
Pt_3Co	AB	2.2	0.8	19015598
Pt_3Co	AA	2.4	1.4	19015598
Pt_3Zn	AB	3.2	1.3	19030163
Pt_3Zn	AA	2.2	1.4	19030163
Pt_3Hf	AB	3.3	-0.6	19066200
Pt_3Hf	AA	2.5	0.4	19066200
Pt_3Nb	AB	2.4	-1.5	19016685
Pt_3Nb	AA	3.0	-1.0	19016685
Pt_3Sc	AB	2.8	-0.3	19170000
Pt_3Sc	AA	1.9	0.7	19170000
Pt_3Ta	AB	2.4	-1.7	19216125
Pt_3Ta	AA	3.1	-1.1	19216125

Alloy	Surface Termination	C [eV]	C [eV]	Price [$/kmol]
Pt_3Ti	AB	2.7	−0.9	19091820
Pt_3Ti	AA	2.6	0.0	19091820
Pt_3V	AB	2.2	−1.3	19040550
Pt_3V	AA	2.7	−0.8	19040550
Pt_3Y	AB	2.5	−0.2	19108175
Pt_3Y	AA	3.2	−0.7	19108175
Pt_3Zr	AB	3.2	−0.7	19030163
Pt_3Zr	AA	2.5	0.4	19030163
Pt_3Sn	AB	4.2	1.7	19019640
Pt_3Sn	AA	2.5	1.4	19019640
Pt_3Ga	AB	2.9	2.3	19051000
Pt_3Ga	AA	2.2	1.4	19051000
Pt_3Ge	AB	3.4	1.1	19078200
Pt_3Ge	AA	2.7	1.4	19078200
Pt_3In	AB	2.8	1.7	19290800
Pt_3In	AA	2.0	1.3	19290800
Pt_3Al	AB	3.0	0.6	19013560
Pt_3Al	AA	2.0	1.0	19013560
Pt_3La	AB	2.0	−0.2	19290500
Pt_3La	AA	1.2	0.7	19290500
Pt_3Cd	AB	3.5	1.7	19025380
Pt_3Cd	AA	1.8	1.3	19025380
Pt_3Pb	AB	3.1	1.9	19013768
Pt_3Pb	AA	2.2	1.3	19013768

Alloy	Surface Termination	C [eV]	C [eV]	Price [$/kmol]
Pt_3Sb	AB	3.2	1.3	19013861
Pt_3Sb	AA	2.3	1.5	19013861
Pt_3As	AB	3.0	1.2	19072500
Pt_3As	AA	1.8	1.2	19072500
Pt_3Tl	AB	2.7	2.0	19036980
Pt_3Tl	AA	1.9	1.3	19036980

6 Alloy Stability

The stability filters as applied in the work on steam reforming MKM by Xu et al. [10] have been used in this study. The thermodynamic stability of alloys has been accessed by the formation energy of the A_3B bimetallic alloy. The energy of alloy formation is given in Table SI-2.

Table SI-2: Alloy Formation Energy and Gibbs Energy of Oxidation

Alloy	Formation Energy[eV]
Pt_3Cu	-0.49
Pt_3Zn	-1.35
Pt_3Ga	-1.81
Pt_3Ge	-1.03
Pt_3Pb	-0.53
Pt_3Sb	-0.75

7 References

[1] Khan T. S.; Jalid F.; Haider M. A., *Top Catal* 2018, 1-12.
[2] Grabow L. C., Computational Catalyst Screening, *RSC Publishing* 2012.
[3] Medford, A. J.; Shi, C.; Hoffmann, M. J.; Bligaard, T.; Nørskov, J. K. *Catal. Lett.* 2015, 794–807.
[4] Medford A. J.; Lausche A. C.; Abild-Pedersen F.; Temel B.; Schjødt N. C., *Top Catal* 2014, l57, 135–142.
[5] Hummelshøj JS, Abild-Pedersen F, Studt F, et al *Angew Chem Int Ed* 2012, 51:272–274.
[6] Peterson, A. A.; Abild-pedersen, F.; Studt, F.; Rossmeisl, J.; Nørskov, J. K. *Energy Environmental Science* 2010, 1311–1315.
[7] Jalid F.; Khan T. S.; Mir F. Q.; Haider M. A., *J. Catal* 2017, 353, 265-273.
[8] Jiang, T.; Mowbray D. J.; Dobrin, S.; Falsig, H.; Hvolbæk, B.; Bligaard, T.; Nørskov, J. K. *J. Phys. Chem. C* 2009, 113, 10548–10553.
[9] Jones G.; Studt F.; Abild-Pedersen F.; Nørskov J. K.; Bliggard T. *Chem Eng Sci* 2011, 66, 6318–6323.
[10] Xu Y.; Lausche, A. C.; Wang, S.; Khan, T. S.; Abild-Pedersen, F.; Studt, F.; Nørskov, J.K.; Bligaard, T. *New J. Phys.* 2013, 15, 125021.